Energy Conversion and Management 62 (2012) 47–50

Contents lists available at SciVerse ScienceDirect

Energy Conversion and Management

journal homepage: www.elsevier.com/locate/enconman

Characterization of a thermoelectric generator at low temperatures

Sevan Karabetoglu, Altug Sisman *, Z. Fatih Ozturk, Turker Sahin

Istanbul Technical University, Energy Institute, 34469 Maslak, Istanbul, Turkey

ARTICLE INFO

Article history:
Received 12 October 2011
Received in revised form 15 March 2012
Accepted 7 April 2012
Available online 25 June 2012

Keywords:
Thermoelectric properties
Thermoelectric generators
Cryogenic characterization
Bi_2Te_3

ABSTRACT

For the low temperature applications of Bi_2Te_3 based thermoelectric power generators (TEGs), determination of low temperature material behaviors is important. In the temperature range of 100–375 K, temperature dependency of Seebeck coefficient and electrical conductivity of a Bi_2Te_3 based TEG are experimentally determined. Furthermore, for a constant temperature difference, the variation of maximum power output with the mean temperature is analytically examined based on the experimentally measured material properties. It is observed that 250 K seems a critical mean operating temperature for the considered Bi_2Te_3 module. Correlations for temperature dependency of material quantities are also given for the temperature region of 100–375 K. The results can be used for the low temperature applications of Bi_2Te_3 based TEGs.

1. Introduction

Thermoelectric devices consist of simple thermocouples which can directly convert either thermal energy into electrical energy for power generation applications or electrical energy into thermal energy for heating or cooling applications. Although thermoelectric devices have many advantages; they are not commonly used due to their lower efficiency and higher costs in comparison with those of the conventional systems. After the recent advances in material science, however, thermoelectric power generator modules with 5% efficiency and Peltier coolers with COP value of 1.5 for 20 °C temperature difference are commercially available. On the other hand, higher efficient (up to 17% for 200 °C temperature difference) TEG modules based on different type of nano-materials have been developed in many research laboratories [1–3,19].

In most of the applications, thermoelectric devices are used for cooling purposes [4–7]. However, thermoelectric generators have also been used in a number of applications such as battery charging [8], waste heat recovery [9,10], power from radioisotopes [11,12], as well as electrification of rural homes [13]. Thermoelectric devices are commonly produced for the operating temperatures ranging from room temperature to higher temperatures. Therefore, there are only a few works in literature on the characteristics and performance of thermoelectric devices at low temperature range [14–17]. Heat energy transfer from environment to the liquefied natural gas (LNG) during its evaporation can be used to generate electricity by TEGs [14]. Therefore evaporation process of liquefied gases constitutes a possibility for the low temperature applications of TEGs.

In this work, a Bi_2Te_3 based thermoelectric power generator is considered since they are commercially available and relatively inexpensive. Its material characteristics such as Seebeck coefficient and electrical conductivity are experimentally determined for low temperature region (100–300 K). Furthermore the variation of maximum electrical power output for a given temperature difference with the mean operating temperature is analyzed by using the experimentally measured material properties in some analytical expressions. The results represent the low temperature characteristics of Bi_2Te_3 based thermoelectric materials. They can be useful for the studies on low temperature engineering applications of TEG modules as well as the material science.

2. Experimental set-up

The schematic diagram of the experimental set-up is shown in Fig. 1. The set-up consists of thermoelectric module which is clamped between two copper plates contacting hot and cold surfaces. The thermoelectric module is surrounded by XPS insulator to reduce heat losses to ambient. For the measurements, temperature, heat flux, current and voltage sensors are used. Uncertainties of voltmeter, ampere meter, thermometer and heat flux meter are ±0.04%, ±1%, ±0.5% and ±3% respectively. K-type thermocouples are used for the temperature measurement of both hot and cold side lead surfaces of TEG module as well as the interfaces between the copper plates and hot and cold plates. The heat flux meters are settled between copper plates and TEG module surfaces. The system also includes the liquid nitrogen vessel at 77 K and electrical heaters to adjust the cold and hot surface temperatures, T_L and T_H respectively.

* Corresponding author. Tel.: +90 212 285 39 39; fax: +90 212 285 38 84.
E-mail addresses: karabetoglu@itu.edu.tr (S. Karabetoglu), sismanal@itu.edu.tr (A. Sisman), ozturkzeh@itu.edu.tr (Z. Fatih Ozturk), turker.sahin@gmail.com (T. Sahin).

0196-8904/$ - see front matter © 2012 Elsevier Ltd. All rights reserved.
http://dx.doi.org/10.1016/j.enconman.2012.04.005

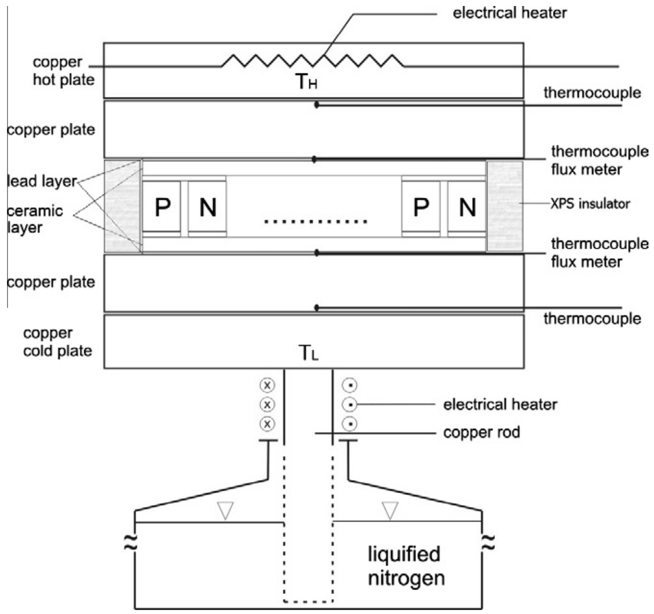

Fig. 1. Schematic diagram of the experimental set-up.

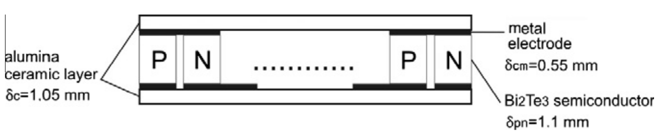

Fig. 2. Schematic cross-sectional view of TEG module.

A commercially available Bi_2Te_3 based thermoelectric generator is chosen. It generates 14.1 W electrical power for hot and cold side temperatures of 250 °C and 50 °C respectively. The overall sizes are 56 mm width, 56 mm length and 4.3 mm height (or thickness). The number of p–n semiconductor couples is N_{pn} = 241. For both p-type and n-type single semiconductors, base sizes are 1.7 mm × 1.7 mm and its thickness is 1.1 mm. The cross-sectional view as well as thicknesses of materials are seen in Fig. 2. Open circuit voltage and short circuit current are 8.4 V and 6.7 A respectively for T_L = 50 °C and T_H = 250 °C.

3. Characterization

During the experiments, the temperature difference between hot and cold surfaces of TEG module is kept constant at 20 K. For ΔT = 20 K temperature difference; generated voltage V, current I, heat fluxes at hot and cold sides ($\dot{q}''_H$ and $\dot{q}''_L$) as well as temperatures T are measured for different electrical load, R_L values practically ranging from zero to infinite ohms. The ambient temperature is set to 25 °C (298 K) and the heat exchange between ambient and the lateral walls of the generator is neglected. Because the lateral surfaces are insulated by XPS material and also the total lateral surface area is too small in comparison with hot and cold side surfaces. Measurements are repeated for different mean temperatures, $\overline{T} = (T_H + T_L)/2$, ranging from 100 K to 375 K. Since the temperature difference is small enough (ΔT = 20 K), temperature dependence of Seebeck coefficient and electrical conductivity are assumed to be linear for this small temperature interval ranging from $T_L = \overline{T} - \Delta T/2$ to $T_H = \overline{T} + \Delta T/2$. In this case, integral averages of these quantities for temperature interval of 20 K are equal to their values at mean temperature. Therefore, open circuit voltage V_o is expressed as

$$V_o = N_{pn}\int_{T_L}^{T_H}\alpha_{np}(T)dT = N_{pn}\int_{\overline{T}-\Delta T/2}^{\overline{T}+\Delta T/2}(A_\alpha + B_\alpha T)dT$$
$$= N_{pn}(A_\alpha + B_\alpha\overline{T})\Delta T = N_{pn}\alpha_{np}(\overline{T})\Delta T. \quad (1)$$

where $\alpha_{np} = \alpha_p - \alpha_n$ is the Seebeck coefficient of a single p–n couple, A_α and B_α are the linear coefficients representing the temperature dependency of the Seebeck coefficient for a small temperature interval. Therefore temperature dependent Seebeck coefficient is simply calculated by measuring the open circuit voltage and temperatures of hot and cold sides as

$$\alpha_{np}(\overline{T}) = \frac{V_o}{N_{pn}\Delta T}. \quad (2)$$

The full derivate of a material quantity (Seebeck coefficient and electrical conductivity) with respect to the measured quantities represents the uncertainty of the material quantity as a function of uncertainties of the measured quantities. By using the linear approximation (small uncertainties), the ratio of the full derivative of the material quantity to its value is assumed to be the value of total percent uncertainty. Therefore, total percent uncertainty of the Seebeck coefficient is calculated from (2) as follows

$$\frac{d\alpha}{\alpha} = \frac{dV_o}{V_o} - \frac{d\Delta T}{\Delta T}. \quad (3)$$

and

$$\Delta_\alpha = \pm\Delta_V \pm \Delta_{\Delta T}. \quad (4)$$

Uncertainty of the measurement of Seebeck coefficient is in order of ±0.54%.

Determination of internal resistance based on simultaneous DC current and voltage measurements causes wrong results since the DC current itself induces a Peltier effect which changes the temperature difference during the measurement. This induced temperature difference changes the net electrical potential difference applied to the material and causes wrong resistance measurement. Therefore to prevent the induction of Peltier effect during the measurement of internal electrical resistance, it is measured by an impedance meter, which uses AC signal. Internal resistance can be expressed as

$$R_i = N_{pn}\left[\frac{1}{\sigma_n}\frac{\delta_n}{A_n} + \frac{1}{\sigma_p}\frac{\delta_p}{A_p} + 2\frac{r_{con}}{A_{con}}\right]. \quad (5)$$

where σ is the electrical conductivity, δ is the thickness, A is the cross sectional area, r_{con} is the contact resistance between metal electrodes and semiconductor p–n couple while the subscripts n and p represent n-type and p-type semiconductors respectively. Here the resistance of metal electrode itself is neglected since the electrical conductivity of metals is too high in comparison with those of semiconductors, $\sigma_e \gg \{\sigma_n, \sigma_p\}$.

In macroscopic thermoelectric devices, electrical contact resistance between the semiconductor and metal electrodes has been reported to typically be between 10^{-8} and 10^{-9} Ω m^2 [18]. In this work, r_{con} is assumed to be 5.10^{-9} Ω m^2 as an average value. Since $\delta_n = \delta_p = \delta_{pn}$ and $A_{con} = A_n = A_p = A_{pn}$ for the considered TEG, (5) can be simplified as

$$R_i \cong N_{pn}\left(\frac{1}{\sigma_n} + \frac{1}{\sigma_p} + \frac{2r_{con}}{\delta_{pn}}\right)\frac{\delta_{pn}}{A_{pn}} = N_{pn}\left(\frac{\sigma_n + \sigma_p}{\sigma_n\sigma_p} + \frac{2r_{con}}{\delta_{pn}}\right)\frac{\delta_{pn}}{A_{pn}}$$
$$= N_{np}\left(\frac{1}{\sigma_{pn}} + \frac{2r_{con}}{\delta_{pn}}\right)\frac{\delta_{pn}}{A_{pn}}. \quad (6)$$

Therefore electrical conductivity of p–n pairs is expressed by

$$\sigma_{pn}(\overline{T}) = \frac{\sigma_n\sigma_p}{\sigma_n + \sigma_p} = \left[\frac{R_i(\overline{T})}{N_{pn}}\frac{A_{pn}}{\delta_{pn}} - \frac{2r_{con}}{\delta_{pn}}\right]^{-1}. \quad (7)$$

Uncertainty of the measurement of electrical conductivity is in order of ±3.5%. It should be noted that the temperature dependencies of electrical conductivity are assumed to be linear for small temperature interval of 20 K during the measurements. Therefore, integral averages of this quantity for 20 K interval are equal to their values at mean temperature, like the Seebeck coefficient given by (2). To make the results more general, dimensionless Seebeck coefficient and electrical conductivity are defined as follows

$$\tilde{\alpha}(T) = \alpha_{np}(T)/\alpha_{np}(T = 300\,\mathrm{K}), \tag{8}$$

$$\tilde{\sigma}(T) = \sigma_{np}(T)/\sigma_{np}(T = 300\ \mathrm{K}). \tag{9}$$

4. Experimental results and discussion

During the experiments ambient temperature is kept at 25 °C (298 K) and the heat exchange between ambient and the lateral walls of TEG is neglected due to the reasons explained in Section 3. Second order polynomial expressions are fitted to the experimental data of the dimensionless Seebeck coefficient and electrical conductivity.

In Fig. 3, it is seen that the Seebeck coefficient of a Bi_2Te_3 p–n couple decreases with decreasing temperature, up to 80% for T = 100 K due to the lack of thermal excitations at lower temperatures. Solid lines represent the expected values while the dots stand for experimental values. The mean absolute percentage error (MAPE) of the solid line is defined as

$$MAPE = \frac{1}{n}\sum_{k=1}^{n}|A_k - P_k|/A_k, \tag{10}$$

where A_k is the actual (experimental) value, P_k is the theoretically predicted value and n is the number of experiments. MAPE value is 4.0% for this figure.

In Fig. 4, the variation of dimensionless electrical conductivity with mean temperature is given. It is seen that electrical conductivity considerably increases with decreasing temperature and it takes nearly 4.5 times higher values at 100 K than the value at 300 K. This is because of the lower probability of collision of electrons and holes with lattice atoms and impurities at lower temperatures. MAPE value of the solid line is 4.5% for this figure.

The measured values of Seebeck coefficient and electrical conductivity of a single Bi_2Te_3 p–n couple at 300 K are α_{pn} = 345 μV/°C and σ_{pn} = 28103 Ω m respectively while they are given as α_{pn} = 382 μV/°C and σ_{pn} = 30239 Ω m in literature [19]. Therefore, the relative differences between the measured quantities and the values given in literature are less than 10% for Seebeck coefficient and 8% for electrical conductivity.

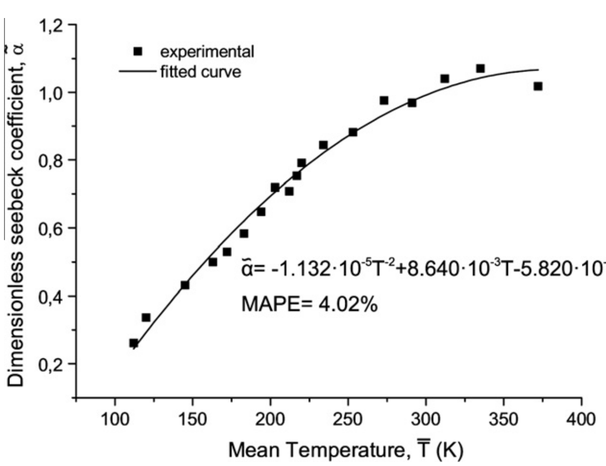

Fig. 3. Variation of dimensionless Seebeck coefficient with mean temperature for ΔT = 20 K.

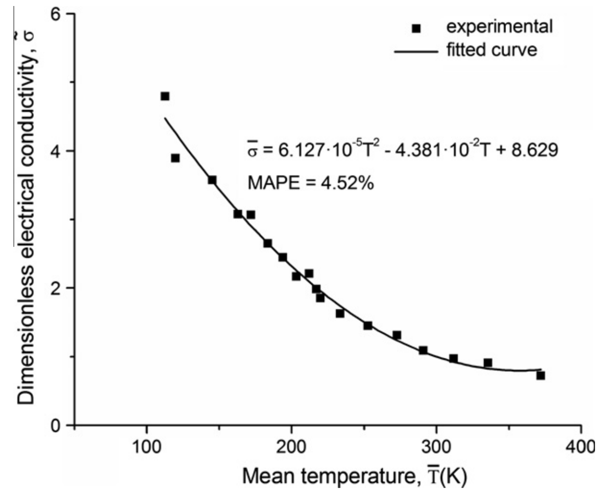

Fig. 4. Variation of dimensionless electrical conductivity with mean temperature for ΔT = 20 K.

5. Examination of maximum power

The variations of the material properties at low temperatures cause the change of behaviors of a commercial TEG module. Maximum power output can be calculated by using the experimentally measured material properties. The calculations are made for the same temperature difference of 200 K, which is the common operating temperature difference for commercial TEGs, and only the mean temperature is changed between 100 K and 375 K. The dimensionless form of maximum power output is defined by dividing the values to the value at mean temperature of 300 K. Maximum power output is expressed as

$$P_{\max}(\overline{T}, \Delta T) = \frac{V_{OC}^2}{4R_i} = \frac{\left[N_{pn}\int_{\overline{T}-\Delta T/2}^{\overline{T}+\Delta T/2}\alpha(T)dT\right]^2}{4\frac{N_{pn}}{A}\frac{\delta_{pn}}{\Delta T}\int_{\overline{T}-\Delta T/2}^{\overline{T}+\Delta T/2}\frac{1}{\sigma_{pn}(T)}dT}. \tag{11}$$

Therefore the dimensionless maximum power output is given by

$$\widetilde{P}_{\max}(\overline{T}, 200) = \frac{P_{\max}(\overline{T}, 200)}{P_{\max}(300, 200)}. \tag{12}$$

It should be noted that the temperature difference is kept constant as ΔT = 200 K while the mean temperature is changed. Maximum power output of TEG decreases with decreasing mean temperature and there is a sharp descent of power output after the mean temperature of 200 K as it seen in Fig. 5. To generate the same electrical power output at mean temperature of 211 K, which corresponds to LNG evaporation application (T_L = −162 °C, T_H = 38 °C), it is necessary to use 1.2 times more TEG modules working at mean temperature of 411 K, which corresponds to standard application (T_L = 38 °C, T_H = 238 °C) for Bi_2Te_3 based TEGs. Similarly, for evaporation of liquid nitrogen application (T_L = −196 °C, T_H = 4 °C) it is necessary to use 1.45 times more TEG modules in comparison with their standard applications. Furthermore, there is a very smooth variation of dimensionless power output between 250 K and 350 K. It is nearly equal to unity for this temperature interval. Therefore 250 K seems a critical mean operating temperature for this particular Bi_2Te_3 module since there is a sharp descent below this point.

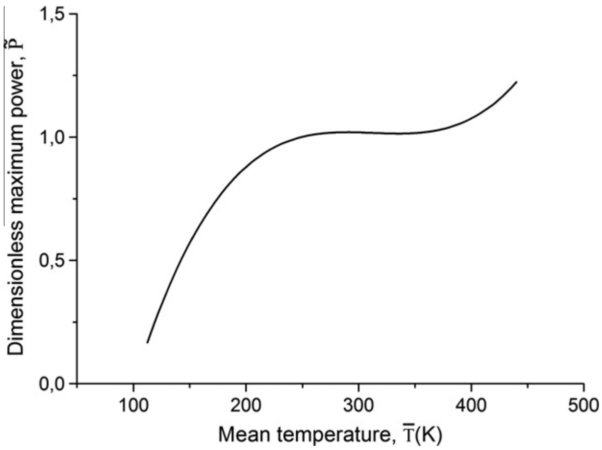

Fig. 5. Dimensionless maximum power output versus mean temperature for $\Delta T = 200$ K.

6. Conclusion

TEGs based on Bi_2Te_3 semiconductors are commercially available and the cheapest versions of thermoelectric generators. Their typical low and high operating temperatures are 50 °C and 250 °C respectively. In this work, temperature dependencies of Seebeck coefficient and electrical conductivity are experimentally determined for low temperature range 100–375 K. Some expressions based on the experimental measurements are given for the temperature dependency of material properties. It is observed that all these results are in a good agreement with the literature [14,16] and [19]. Furthermore, by using the experimentally measured material properties, maximum electrical power output of a Bi_2Te_3 based TEG module is analyzed for low temperature region. It seems that mean operating temperature of 250 K constitutes a critical temperature for this particular thermoelectric generator module. Below this point, it is necessary to use more TEG modules for the same power output. The number of excess thermoelectric modules rapidly increases especially below 200 K. The results can be used for the low temperature applications of Bi_2Te_3 based TEGs.

Acknowledgments

This research project has been financially supported by Drotel Telecommunication Inc. Corp., Ericom Telecommunication and Energy Technologies Inc. Corp. and Istanbul Technical University Scientific Research Project Fund. Authors are grateful for these financial supports.

References

[1] Pei Y, Lensch-Falk J, Toberer ES, Medlin DL, Snyder GJ. High thermoelectric performance in PbTe due to large nanoscale Ag_2Te precipitates and La doping. Adv Funct Mater 2011;21:241–9.
[2] Jovanociv V, Ghamaty S, Krommenhoek D, Bass JC. High coefficient of performance quantum well thermoelectric nano-cooler. Vancouver, British Columbia, Canada: ASME InterPACK; 2007.
[3] Ghamaty S, Elsner NB, Jovanociv V. Thermoelectric quantum well energy harvesting device. In: Energy nanotechnology international conference, Massachusetts Institute of Technology (MIT), Cambridge, USA; 2006.
[4] Zhang HY, Mui YC, Tarin M. Analysis of thermoelectric cooler performance for high power electronic packages. Appl Therm Energy 2010;30:561–8.
[5] Pan Y, Lin B, Chen J. Performance analysis and parametric optimal design of an irreversible multi-couple thermoelectric refrigerator under various operating conditions. Appl Energy 2007;84:882–92.
[6] Min G, Rowe DM. Experimental evaluation of prototype thermoelectric domestic refrigerators. Appl Energy 2006;83:133–52.
[7] Huang BJ, Chin CJ, Duang CL. A design method of thermoelectric cooler. Int J Refrig 2000;23:208–18.
[8] Eakburanatwat J, Boonyaroonate I. Development of a thermoelectric battery-charger with microcontroller-based maximum power point tracking technique. Appl Energy 2006;83:687–704.
[9] Crane DT, Jackson GS. Optimization of cross flow heat exchangers for thermoelectric waste heat recovery. Energy Convers Manage 2004;45:1565–82.
[10] Hsu CT, Huang GY, Chu HS, Yu B, Yao DJ. Experiments and simulations on low-temperature waste heat harvesting system by thermoelectric power generators. Appl Energy 2011;88:1291–7.
[11] Lange RG, Carroll WP. Review of recent advances of radioisotope power systems. Energy Convers Manage 2008;49:393–401.
[12] O'Brien RC, Ambrossi RM, Bannister NP, Howe SD, Atkinson HV. Safe radioisotope thermoelectric generators and heat sources for space applications. J Nucl Mater 2008;377:506–21.
[13] Rinalde GF, Juanico LE, Taglialavore E, Gortari S, Molina MG. Development of thermoelectric generators for electrification of isolated rural homes. Int J Hydrogen Energy 2010;35:5818–22.
[14] Sun W, Hu P, Chen Z, Jia L. Performance of cryogenic thermoelectric generators in LNG cold energy utilization. Energy Convers Manage 2005;46:789–96.
[15] Chung DY, Hogan T, Brazis P, Lane MR, Kannewurf C, Bastea M, et al. $CsBi_4Te_6$: a high-performance thermoelectric material for low-temperature applications. Science 2000;287:1024–7.
[16] Harutyunyan SR, Vardanyan VH, Kuzanyan AS, Nikoghosyan VR, Kunii S, Wood KS, et al. Thermoelectric cooling at cryogenic temperatures. Appl Phys Lett 2003;83:2142–4.
[17] Sivapurapu SVK. Preliminary design of a cryogenic thermoelectric generator. M.Sc. dissertation. Texas, USA: University of North Texas; 2007.
[18] da Silva LW, Kaviany M. Micro-thermoelectric cooler: interfacial effects on thermal and electrical transport. Int J Heat Mass Transfer 2004;47:2417–35.
[19] Rowe DM. Thermoelectrics handbook macro to nano. New York: Taylor & Francis Group, LLC; 2006 [p. 9/14–16 and 57/1–11].